

High-pressure elastic properties of liquid and solid krypton to 8 GPa

H. Shimizu, N. Saitoh, and S. Sasaki

Department of Electronics, Gifu University, 1-1 Yanagido, Gifu 501-11, Japan

(Received 4 April 1997)

The direction-dependent acoustic velocities, refractive index, adiabatic elastic constants, adiabatic bulk modulus, and elastic anisotropy in liquid and solid krypton have been determined under pressures up to 8 GPa by Brillouin spectroscopy, with *in situ* identification of the krypton single-crystal orientation in a diamond-anvil cell. Typical values of the three adiabatic elastic constants for fcc crystalline krypton are $C_{11}=40.7$, $C_{12}=28.7$, and $C_{44}=15.8$ GPa at 6 GPa and room temperature. These results contrast fundamentally with the inequality $C_{11}>C_{44}>C_{12}$ determined previously over the same pressure range. The elastic anisotropy, $A=3.3$ at 1 GPa, shows a gradual decrease to 2.5 at 8 GPa. These properties are compared with those of solid methane, which undergoes molecular rotation. [S0163-1829(98)02901-4]

I. INTRODUCTION

Krypton (Kr) is the simplest molecular material, and its condensed phases are of fundamental importance for model calculations of rare-gas solids. At atmospheric pressure, krypton liquefies at about 119.6 K and solidifies in the face-centered cubic (fcc) phase at about 116.4 K. At room temperature, liquid Kr crystallizes into the same phase at about 0.83 GPa.¹ This rare-gas van der Waals solid can be treated as a standard for comparisons with fcc molecular crystals²⁻⁴ showing molecular rotations, because monatomic solid Kr does not contain rotating molecules.

Landheer *et al.*⁵ measured the Brillouin scattering of single-crystal Kr at 115.6 K and atmospheric pressure, and determined three elastic constants C_{11} , C_{12} , and C_{44} . Polian *et al.*⁶ determined the equation of state and elastic properties of solid krypton at pressures up to 30 GPa and room temperature by using energy-dispersive x-ray diffraction and Brillouin scattering, respectively. By Brillouin spectroscopy of the longitudinal acoustic (LA) mode using a backscattering geometry, they measured the pressure dependence of $n\nu$ (n ; refractive index, ν ; LA velocity) for arbitrary unknown directions of a Kr single-crystal without identification of the crystal orientations. In this manner, they determined the effective elastic constants by using the density from x-ray diffraction, deriving three elastic constants and the refractive index.

Recently, we have determined the pressure dependence of three adiabatic elastic constants of solid methane (CH₄) up to 5 GPa.⁴ It has the fcc structure, a closed-shell spherical electronic configuration, and the weak van der Waals forces, which characterize the rare-gas solids. The result, however, exhibits some strikingly different elastic properties compared to the rare-gas family.

In this paper, we present acoustic velocities for all directions, deriving the refractive index, three adiabatic elastic constants (C_{11} , C_{12} , and C_{44}), adiabatic bulk modulus (B_S), and elastic anisotropy of liquid and solid krypton at pressures up to 8 GPa. These properties were all determined by using Brillouin scattering measurements with *in situ* identification of the crystal orientation at each pressure. The results are compared with those of the earlier studies by Landheer

*et al.*⁵ at low temperature and by Polian *et al.*⁶ at high pressures, and the origin of the discrepancy with earlier high-pressure results is investigated. The significant feature of the Kr elastic anisotropy is discussed in comparison with the rare-gas family,^{1,7} as well as solid methane⁴ that contains rotating molecules.

II. EXPERIMENT

To load Kr in a diamond-anvil cell (DAC), we condensed commercial gaseous Kr by spraying its vapor into the gasket hole of the DAC cooled in liquid nitrogen. When the hole was full of solidified Kr, the upper diamond was translated to seal the sample. After adequate pressure had been applied, the DAC was warmed to room temperature.⁸ A single crystal of Kr was grown by increasing the pressure on a seed crystal, which coexists with the liquid at 0.90 GPa. This value is close to the melting line.¹ No pressure transmitting medium was used. The pressure was measured by the ruby-scale method.

For Brillouin measurements, the 514.5 nm argon-ion laser line (λ_0) with a single longitudinal mode was used with an input power level of about 100 mW. The heart of the apparatus was a Sandercock tandem Fabry-Perot interferometer,⁹ which was used in a triple-pass arrangement. The Brillouin frequency shifts ($\Delta\nu$) at 90° and 180° scattering geometries with the DAC (angles between incident and scattered beams) are related to the acoustic velocity (ν) as follows:¹⁰

$$\Delta\nu_{90} = \sqrt{2}\nu_{90}/\lambda_0 \quad (1)$$

and

$$\Delta\nu_{180} = (2n)\nu_{180}/\lambda_0, \quad (2)$$

where the wave vector \mathbf{q} of the acoustic phonons is parallel (90°) and perpendicular (180°) to the interfaces of the input and output diamonds crossed by the laser beam, and ν_{90} is independent of the refractive index of the medium.

III. RESULTS AND DISCUSSION

We determined the pressure dependence of acoustic velocity and refractive index for liquid Kr at pressures up to

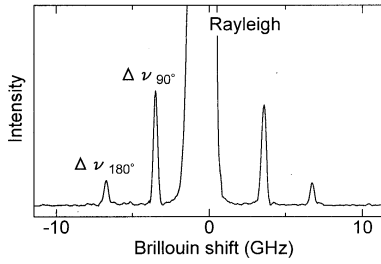


FIG. 1. Brillouin spectrum of liquid Kr at $P=0.59$ GPa. $\Delta\nu_{90^\circ}$ and $\Delta\nu_{180^\circ}$ are Brillouin-shifted signals from 90° and 180° scattering, respectively.

0.90 GPa and 300 K. A typical Brillouin spectrum of liquid Kr ($P=0.59$ GPa) at 90° scattering geometry is shown in Fig. 1. We can observe Brillouin frequency shifts for $\Delta\nu_{90^\circ}$ and $\Delta\nu_{180^\circ}$ simultaneously, because the laser beam reflected from the output diamond serves as an incident beam, giving the weak 180° scattering signal.^{10,11} Figure 2 shows the pressure dependence of $\Delta\nu_{90^\circ}$, $\Delta\nu_{180^\circ}$, and the sound velocity (v_{90°) from Eq. (1) below $P=0.90$ GPa. Because the liquid is acoustically isotropic, the sound velocity is the same for all directions. Therefore, we can determine the pressure dependence of n by using the ratio of $\Delta\nu_{90^\circ}$ to $\Delta\nu_{180^\circ}$, $\Delta\nu_{90^\circ}/\Delta\nu_{180^\circ}=1/(\sqrt{2}n)$ (see solid circles in Fig. 3). The refractive index increases sharply with pressure and has, near the solidification point, a value of about 1.38, which is comparable to that of H_2O at $P=0.1$ MPa and room temperature.

For solid Kr at pressures between 0.90 and 8 GPa, the acoustic and elastic properties have been studied by using the method of high-pressure Brillouin spectroscopy recently developed for simple molecular solids.^{12,13} A typical Brillouin spectrum of solid Kr at 1.66 GPa is shown in Fig. 4. LA and two transverse (TA_1, TA_2) modes are clearly observed. Brillouin measurements at 90° scattering geometry were made in 10° intervals of rotation angle ϕ about the load axis of the DAC in the laboratory frame. The observed Brillouin frequency shifts, that is, acoustic velocities at 1.66 GPa, are plotted as a function of ϕ as open circles in Fig. 5. To analyze the angular dependence of the sound velocities for the LA and two TA_1 (slow) and TA_2 (fast) modes at each pressure, we used Every's expressions¹⁴ relating acoustic velocities for an arbitrary direction to the elastic constants (C_{ij}). The velocities can therefore be expressed as a function of six parameters: $v_j = g_j (C_{11}/\rho, C_{12}/\rho, C_{44}/\rho, \theta, \phi, \chi)$,³ where

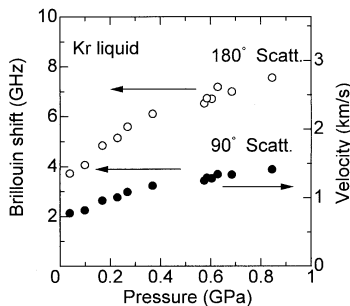


FIG. 2. Pressure dependence of Brillouin frequency shifts at 90° and 180° scatterings for liquid Kr. Solid circles (90° scattering) indicate acoustic velocity simultaneously.

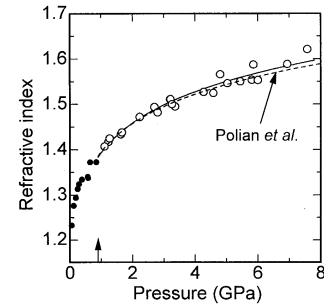


FIG. 3. Pressure dependence of the refractive indices (n) for liquid Kr (solid circles) and solid Kr (open circles) at 300 K. The vertical arrow indicates the liquid-solid phase transition point at $P=0.90$ GPa. The solid line represents a least-squares fit to the present results, and the dashed line shows the result by Polian *et al.* (Ref. 6).

the subscript j indicates LA, TA_1 , and TA_2 modes, ρ is density, and (θ, ϕ, χ) are the Euler angles relating the laboratory frame (DAC) to the crystal reference frame. A least-squares fit was applied to determine acoustic velocities and elastic constants of the fcc Kr single-crystal at each pressure. We found excellent agreement between the measured and the fitted values, as seen in Fig. 5. The best fitting results yielded $C_{11}/\rho=3.96$, $C_{12}/\rho=2.94$, and $C_{44}/\rho=1.54 \text{ km}^2 \text{ s}^{-2}$ at $P=1.66$ GPa. An independent procedure for different crystal orientations showed consistency for these values within an accuracy of $\pm 2\%$. The crystal orientations grown in the DAC, which were determined from the best fitted Euler angles, were typically with (100) or (111) crystallographic planes along the diamond interfaces.

Once the six parameters were determined, the acoustic velocities could be calculated for all directions. Figure 6 shows the Kr sound velocities for typical directions as a function of pressure up to 8 GPa at 300 K. At the freezing point ($=0.90$ GPa), the sound velocity shows a discontinuous change to the LA, TA_2 , and TA_1 velocities in the solid phase of Kr, and these increase with pressure. Furthermore, we can calculate the sound velocity (v_{180°) along the direction perpendicular to the diamond interfaces, which allows us to determine the refractive index (n) by using Eq. (2). From the $\Delta\nu_{180^\circ}$ measured at 180° scattering geometry, we can obtain the pressure dependence of n for solid Kr as shown in Fig. 3. The refractive index is almost continuous across the freezing point, probably due to the van der Waals solid being a simple closed-shell insulator. The n of solid Kr shows a gradual increase with pressure, from $n=1.40$ at 1 GPa to $n=1.60$ at 8 GPa. The present results are in good

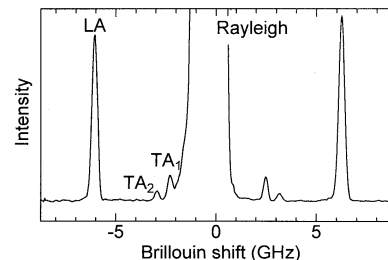


FIG. 4. Brillouin spectrum of solid Kr at $P=1.66$ GPa. LA, TA_2 , and TA_1 are Brillouin-shifted signals from longitudinal, fast, and slow transverse modes, respectively.

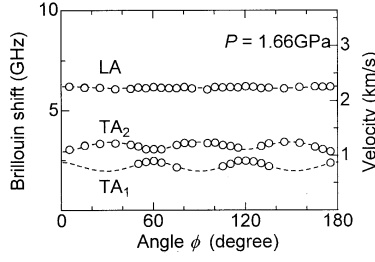


FIG. 5. Brillouin frequency shifts and acoustic velocities of LA, TA₂, and TA₁ modes as a function of angle ϕ at a 90° scattering geometry for solid Kr at $P=1.66$ GPa. The ϕ shows the rotation angle about the load axis of DAC. Open circles indicate experimental points, and the dashed line represents the calculated best-fit velocities.

agreement with those obtained by Polian *et al.*⁶

In Fig. 7 we show the pressure dependence of the three adiabatic elastic constants and the adiabatic bulk modulus [$B_S=(C_{11}+2C_{12})/3$], which were determined from the best-fitted results for C_{ij}/ρ with the pressure dependence of ρ from x-ray studies.⁶ Typical values at $P=6$ GPa and 300 K are as follows: $C_{11}=40.7$, $C_{12}=28.7$, $C_{44}=15.8$ GPa, and $B_S=32.7$ GPa. The low-temperature solid⁵ shows $C_{11}=2.66$, $C_{12}=1.73$, $C_{44}=1.26$ GPa, and $B_S=2.04$ GPa at $T=115.6$ K and $P=0.1$ MPa. The ratios (high pressure/low temperature) all yield roughly the same value: C_{11} , $40.7/2.66=15.3$; C_{12} , $28.7/1.73=16.5$; C_{44} , $15.8/1.26=12.5$; and B_S , $32.7/2.04=16.0$. Previous results for the high-pressure solid⁶ are, for example, $C_{11}=43$, $C_{12}=19$, $C_{44}=23$ GPa, and $B_S=27$ GPa at $P=6$ GPa and room temperature. The agreement for the value of C_{11} is good. However, the result $C_{11}>C_{44}>C_{12}$ contrasts fundamentally with our inequality $C_{11}>C_{12}>C_{44}$. Furthermore, the previous determinations of C_{12} and C_{44} as a function of pressure showed a crossover around $P=14$ GPa,⁶ whereas, the present results show that this is unlikely (Fig. 7).

Let us investigate the origin of the disagreement between our present results and the earlier high-pressure results of Polian *et al.*⁶ They measured the pressure dependence of the LA velocity for arbitrary unknown directions of a Kr single crystal without identifying the crystal orientation, and estimated an envelope for all the experimental points (see Fig. 5 in Ref. 6). The envelope corresponds to maximum and the minimum LA velocities, $v^2=[(C_{11}+2C_{12}+4C_{44})/3]/\rho$ and

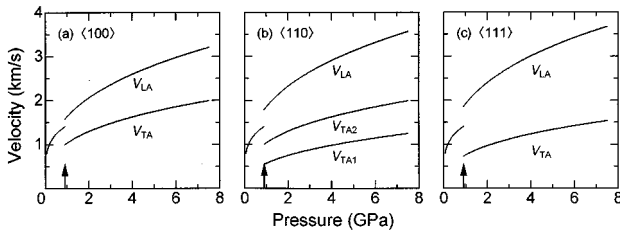


FIG. 6. Pressure dependence of acoustic velocities for liquid and solid Kr at 300 K. The vertical arrows indicate the freezing point ($P=0.90$ GPa). In the fcc solid phase, the velocities for typical directions are shown: (a) $\langle 100 \rangle$, (b) $\langle 110 \rangle$, and (c) $\langle 111 \rangle$ directions. LA, TA₂, and TA₁ are longitudinal, fast, and slow transverse modes, respectively.

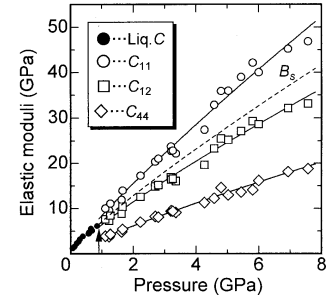


FIG. 7. Pressure dependence of adiabatic elastic constants, C_{11} , C_{12} , and C_{44} for solid Kr at 300 K (open symbols). For the liquid phase (solid circles), the elastic modulus is $C=\rho v^2$. The dashed line indicates the adiabatic bulk modulus (B_S). The vertical arrow indicates the liquid-solid phase transition point at $P=0.90$ GPa.

$v^2=C_{11}/\rho$ along $\langle 111 \rangle$ and $\langle 100 \rangle$ directions, respectively. For the determination of the three elastic constants, they used the isothermal bulk modulus (B_T) obtained by x-ray-diffraction measurements at various pressures. Then, they assumed that the ratio of the specific heats at constant pressure to constant volume, $C_P/C_V=B_S/B_T=\gamma$ is equal to 1, that is, $B_T=B_S=(C_{11}+2C_{12})/3$.

We now discuss the problems with their procedure and justify our own results. (1) They estimated the envelope of velocities from their measured ρv^2 , assuming that the orientation of the crystals formed in the DAC were perfectly random. The minimum curve, as seen in Ref. 6, is reliable because of the large number of data points. However, the maximum curve seems less reliable because of the overestimate at pressures between 3 and 20 GPa, as seen clearly in Ref. 6. The former indicates good agreement between the present and the earlier results for the value of C_{11} , and the latter suggests an overestimate for the value of $2C_{12}+4C_{44}$. (2) They assumed $\gamma=B_S/B_T=1$. Generally, simple molecular solids γ is larger than 1, and decreases to 1 with increasing pressure.^{8,10,15} The ratio of our B_S from Brillouin measurements to their $B_T(=B_S)$ from x-ray studies gives $\gamma=1.34$ at 1 GPa, and decreases to $\gamma=32.7/27=1.21$ at 6 GPa: a reasonable behavior.^{8,10,15} Therefore, we believe that Polian *et al.*'s adiabatic bulk modulus $B_S=(C_{11}+2C_{12})/3$ is underestimated; specifically, the value of C_{12} is underestimated. Consequently, their value of C_{44} becomes overestimated, resulting in their inequality $C_{11}>C_{44}>C_{12}$. Accordingly, we consider our own result $C_{11}>C_{12}>C_{44}$ to

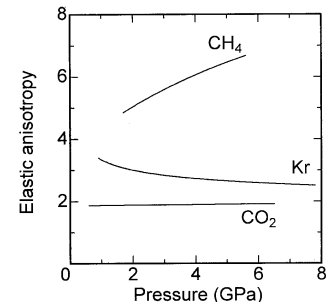


FIG. 8. Pressure dependence of elastic anisotropy [$A=2C_{44}/(C_{11}-C_{12})$] for pressure-induced crystalline Kr, CH₄ (Ref. 4), and CO₂ (Ref. 15) at room temperature.

be more reasonable because it was determined by Brillouin spectroscopy with *in situ* identification of the Kr single-crystal orientation inside the DAC.

The elastic anisotropy A is defined as the square of the ratio of acoustic velocities, TA_2 to TA_1 propagating along the $\langle 110 \rangle$ direction, and is given by the three elastic constants C_{11} , C_{12} , and C_{44} :

$$A = 2C_{44}/(C_{11} - C_{12}). \quad (3)$$

Figure 8 compares the pressure dependence of A for the rare-gas solid Kr, with those of crystalline CH_4 and CO_2 . For solid CH_4 that has molecular rotation, the increase of A with pressure is caused by rotation-translation coupling in the orientationally disordered phase I.⁴ On the other hand, the value of A for solid CO_2 is about 1.9, almost independent of pressure:¹⁵ a behavior typical of most solids. Solid Kr exhibits $A = 3.3$ at $P = 1$ GPa, and shows a gradual decrease to 2.5 at 8 GPa. This trend seems to be characteristic of the simple closed-shell insulator of the rare-gas solid Kr.

Namely, the decrease of A with pressure is probably due to the gradual decrease in space for large variations of the anisotropy under increasing compression.

In conclusion, we have presented systematic studies of Brillouin measurements for liquid and solid phases of the rare-gas Kr at pressures up to 8 GPa and room temperature. The results were compared with earlier Brillouin studies for the low-temperature solid at 0.1 MPa, and for the high-pressure solid at room temperature. The present experimental results for acoustic velocity, refractive index, adiabatic elastic constants, adiabatic bulk modulus, and elastic anisotropy as a function of pressure provide data for high-pressure science and for model calculations of simple rare-gas solids.

ACKNOWLEDGMENTS

We thank T. Kume for his constructive comments. This work was supported by CREST (Core Research for Evolutional Science and Technology) of Japan Science and Technology Corporation.

¹R. K. Crawford, in *Rare Gas Solids*, edited by J. A. Venables and M. L. Klein (Academic, New York, 1976), Vols. I and II.

²S. C. Rand and B. P. Stoicheff, *Can. J. Phys.* **60**, 287 (1982).

³H. Shimizu and S. Sasaki, *Science* **257**, 514 (1992).

⁴H. Shimizu, N. Nakashima, and S. Sasaki, *Phys. Rev. B* **53**, 111 (1996).

⁵D. Landheer, H. E. Jackson, R. A. McLaren, and B. P. Stoicheff, *Phys. Rev. B* **13**, 888 (1976).

⁶A. Polian, J. M. Besson, M. Grimsditch, and W. A. Grosshans, *Phys. Rev. B* **39**, 1332 (1989).

⁷J. Skalyo, Y. Endoh, and G. Shirane, *Phys. Rev. B* **9**, 1797 (1974).

⁸H. Shimizu, in *High Pressure Research on Solids*, edited by M. Senoo *et al.* (Elsevier, Netherlands, 1995), pp. 1–17.

⁹R. Mock, B. Hillebrands, and R. Sandercock, *J. Phys. E* **20**, 656 (1987).

¹⁰H. Shimizu, E. M. Brody, H. K. Mao, and P. M. Bell, *Phys. Rev. Lett.* **47**, 128 (1981).

¹¹E. M. Brody, H. Shimizu, H. K. Mao, P. M. Bell, and W. A. Bassett, *J. Appl. Phys.* **52**, 3583 (1981).

¹²H. Shimizu, M. Ohnishi, S. Sasaki, and Y. Ishibashi, *Phys. Rev. Lett.* **74**, 2820 (1995).

¹³H. Shimizu, T. Nabetani, T. Nishiba, and S. Sasaki, *Phys. Rev. B* **53**, 6107 (1996).

¹⁴A. G. Every, *Phys. Rev. Lett.* **42**, 1065 (1979).

¹⁵H. Shimizu, T. Kitagawa, and S. Sasaki, *Phys. Rev. B* **47**, 11 567 (1993).